Research Article

Received: 10 June 2022 Revised: 1 September 2022 Accepted article published: 4 September 2022 Published online in Wiley Online Library:

(wileyonlinelibrary.com) DOI 10.1002/jctb.7231

Self-supported single-wall carbon nanotube buckypaper membranes applied to air and water filtration

Víctor Berned-Samatán,[a,b] Santiago Jiménez,[c] César Rubio,[a,b] Carlos Téllez[a,b] and Joaquín Coronas[a,b*]

Abstract

Background: This work addresses the use of self-supported single-wall carbon nanotube (SWCNT) buckypapers as filters or membranes to treat air or water streams to reduce the concentration of pollutants.

Results: The fabrication of the buckypapers was carried out by a facile filtration method. The performance of the buckypaper as an air filter was tested with a NaCl aerosol obtaining a permeance of 241 $m^3\ m^{-2}\ h^{-1}\ bar^{-1}$ and a filtration efficiency of 99.9991%. The performance of the buckypaper as a water ultrafiltration (UF) membrane was studied separating ZIF-8 nanoparticles of 30, 50 and 120 nm in diameter, achieving a permeance of 124 $L{\cdot}m^{-2}\ h^{-1}\ bar^{-1}$ and a rejection of 99.99%.

Conclusions: A simple technique is described for the rapid fabrication of self-supported SWCNT buckypaper membranes with a filtration method resulting in an excellent performance in both air and water filtration. In addition, because of the acquired control of ZIF-8 crystallization, particles of different sizes of this material were synthesized *ad hoc* to serve as a reference solute of UF separation.

Supporting information may be found in the online version of this article.

Keywords: single-wall carbon nanotube; buckypaper membrane; aerosol; nanoplastic; water ultrafiltration

INTRODUCTION

Nowadays, the presence of colloidal particles, particularly in the form of nanoplastics,[1] as water pollutants and the aerosol pollution caused by road traffic and industries have become a serious concern due the impact on living environment[2-6] and public health.[7] In fact, among the various types of air pollution, particulate matter (PM) is one of the most serious threats to human health because it can affect the lungs and even alveolar cells.[8] The size of this PM determines the hazards of its respiration and can be categorized according to its aerodynamic diameter in PM_{10} (≤10 μm), $PM_{2.5}$ (≤2.5 μm) and $PM_{0.1}$ (≤0.1 μm).[9,10] One of the most effective ways to decrease the concentration of PM is with filters. While the larger particles (PM_{10}) can be easily removed with air cleaners like cyclones and sedimentation tanks, the more dangerous fine ($PM_{2.5}$) and ultrafine ($PM_{0.1}$) particles require a high-efficiency particulate air filter which must reach an efficiency of 99.97% for 0.3 μm particles.[11] The most important parameters for assessing the performance of a gas filter are the filtration efficiency and the pressure drop.[12,13] A good filter is expected to show a low pressure drop and a high filtration efficiency. The filtering efficiency (E) is calculated with Eqn (1):

$$E = 100 \times \left(1 - \frac{C_p}{C_u}\right) \quad (1)$$

where C_p and C_u are the particle concentrations downstream and upstream of the filter, respectively, and where the ratio C_p/C_u corresponds to P (see Eqn (2)).

The performance of a filter is mainly characterized by the quality factor (QF) which is calculated with Eqn (2)[14,15]:

$$QF = \frac{\ln\left(C_u/C_p\right)}{\Delta p} = \frac{\ln\left(1/P\right)}{\Delta p} \quad (2)$$

* *Correspondence to: J Coronas, Institutode Nanociencia y Materiales de Aragón (INMA), CSIC-Universidad de Zaragoza. c/ Mariano Esquillor, s/n. Zaragoza 50018, Spain. E-mail: coronas@unizar.es*

a *Instituto de Nanociencia y Materiales de Aragón (INMA), CSIC-Universidad de Zaragoza, Zaragoza, Spain*

b *Chemical and Environmental Engineering Department, Universidad de Zaragoza, Zaragoza, Spain*

c *Laboratory of Research in Fluid Dynamics and Combustion Technologies (LIFTEC), CSIC-Universidad de Zaragoza, Zaragoza, Spain*

where P is the penetration rate of particles, that is, the ratio between the concentration of particles downstream (C_p) of the filter and the concentration of particles upstream (C_u), and Δp is the pressure drop across the filter. The higher the QF value the better the expected filter performance.

Filters are usually composed of fibers rendering high porosity and inter-fiber distances larger than the size of the particles to be filtered that causes clogging of the filter. This results in a high increase of pressure drop and the filters have to be disposed of due to their limited service life. Recently, nanofibers have become of interest for the manufacture of air filters due to their high specific surface area and a diameter comparable to that of the mean free path of air molecules (66 nm).[16] This means that theoretically they will have a high efficiency, a low tendency to clogging and thus a low pressure drop overcoming the trade-off between efficiency and pressure drop parameters. Usually these nanofibers are polymer-based; however, carbon nanotubes (CNTs) are very promising materials for building air filters because of their regular diameters in the nanometer range, high porosity and specific surface area, hydrophobicity, inertness and potential functionalization. CNTs are one type of the variety of carbon materials that already exist for water and air applications (activated carbon, graphene, carbon nanofiber, biochar, carbon aerogel). Carbon materials are used as adsorbents for the removal of dangerous and hazardous compounds.[17,18] Besides, CNTs have numerous applications in medicine (carrier for drug delivery, lubricant in tablet manufacturing), artificial implants, preservatives (antioxidant nature), diagnostics (biosensors) and catalysis.[19] In particular, single-walled CNTs (SWCNTs) have attracted interest for this purpose due to their adequate properties in line with those just mentioned. Their high porosity and specific surface area[20] make them a good choice for air[21] and water[22] pollution filtration. The common fabrication method for CNT-based air filters includes coating CNT films on microfiber filters[13] or *in situ* growth of CNTs on filter supports.[23] These supports would have much higher porosity than those generated from the CNTs.

Along with air pollution, the abatement of water pollution is becoming more and more worrying and challenging because industrial and urban activities generate various types of pollution and decrease the quality of water even if every year the regulations for the disposal of wastewater become stricter. In consequence, clean water is predicted to become one of the most precious resources at the end of the century.[24] Pressure-driven membrane processes, that recently have been proposed for remediation of pollution due to the presence of nanoplastic and microplastic particles in water,[1] can be classified in four categories according to the size of solute regularly processed: microfiltration (MF, 100 nm–1 μm), ultrafiltration (UF, 10–100 nm), nanofiltration (NF, 1–10 nm) and reverse osmosis (RO, ≤1 nm).[25] In fact, these dimensions are quite restrictive when compared with the size of the so-called microplastics (in the 0.06–10 mm range).[1] However, plastic pollution may appear in the form of nanoplastics (i.e. particles in the 0.1–2 μm range)[26,27] and also microplastics may evolve by degradation into nanoplastics, sizes that may require the action of a UF membrane separation process.

Having said the above, CNT-based membranes are also popular for water treatment,[28,29] as they combine the performance of traditional membrane materials with the special features of CNTs, like high specific surface area, mechanical strength, chemical inertness, hydrophobicity and water transport.[30,31] Some of the applications of these membranes are in water desalination,[32,33] oil–water separation,[34] removal of heavy metal ions[35] and removal of emerging pollutants[36] and microplastics due the non-polar interaction between them and the CNTs when they act as adsorbates.[29]

In the work reported here, we used a feasible method to obtain self-supported SWCNT buckypaper membranes by vacuum filtration. CNT buckypapers are free-standing sheets of entangled CNTs forming a flexible structure that is physically and chemically stable.[37,38] Such membranes were applied to the removal of aerosols from air and water filtration of the metal–organic framework (MOF) ZIF-8. MOFs are crystalline materials formed by metal clusters and organic linkers which exhibit high surface area and tunable and flexible pore structure.[39,40] Zeolitic imidazolate frameworks (ZIFs) and in particular ZIF-8 show promising abilities for their use in biomedicine due their high pore volume and stability, which have opened the opportunity for the encapsulation and protection of bioactive molecules.[41] ZIF-8 consists of a metal cation of Zn^{2+} coordinated with 2-methylimidazolate forming a SOD-type topology with 1.16 nm cavities connected through 0.34 nm pore windows.[42] Even though MOF stability and toxicity have been found acceptable for biomedical applications,[43] there are studies showing hematotoxicity of ZIF-8, one of the most used MOFs for these kinds of applications.[44] Also, the removal of MOFs from water is of great interest in line with their potential environmental pollution[45] and toxicity due their possible degradation in water, which would release their constituent metal ions and the organic linkers.[46] Moreover, because of the particle size control of ZIF-8 crystallization, this material can serve as a reference UF solute in the range of a few tens of nanometers (e.g. simulating a nanoplastic). To the best of our knowledge, this is the first time that a MOF has been used with this double purpose (pollutant and specialized solute) in membrane filtration operations.

EXPERIMENTAL

Materials

SWCNTs (≥93% carbon content, 1.2–2 nm in diameter) and non-ionic surfactant Triton X-100 were purchased from Sigma-Aldrich. 2-Propanol was purchased from Panreac AppliChem. Nylon filter with a diameter of 47 mm and 0.22 μm pore size was purchased from Labbox. Zinc nitrate hexahydrate (reagent grade) and methanol (MeOH; HPLC grade, ≥99.9%) were purchased from Scharlab and 2-methylimidazole (mIm) (99%) from Acros Organics.

CNT buckypaper preparation

The preparation of free-standing SWCNT films via a vacuum filtration method was achieved adapting a previously reported method.[47,48] Typically, 10 mg of SWCNTs was dispersed into 1 wt% of Triton X-100 surfactant in 60 mL of distilled water. The obtained suspension was treated by ultrasound using a probe sonicator (Sonics Materials VC-750-220, 750 W, 20 kHz) for 1 h. The sonicated suspension was then filtered through a porous Nylon filter placed in a 47 mm diameter glass filtration funnel and washed with a mixture of acetone and 2-propanol.[47] Under such conditions, a 15 μm thick, self-standing SWCNT buckypaper was obtained. This was dried overnight at room temperature after which it could be peeled off from the Nylon filter.

Synthesis of ZIF-8 nanoparticles

ZIF-8 nanoparticles with various sizes (30, 50 and 120 nm) were synthesized by previously reported methods.[49,50] Briefly, two solutions, one of the metal salt and another of the ligand, were prepared with half of the total MeOH for each solution.

Journal of Chemical Technology and Biotechnology published by John Wiley & Sons Ltd on behalf of Society of Chemical Industry (SCI).

Then the two solutions were mixed resulting in final molar compositions of 500:1:8 MeOH:Zn^{2+}:mIm (120 nm), 1000:1:8 MeOH:Zn^{2+}:mIm (50 nm) and 1500:1:8 MeOH:Zn^{2+}:mIm (30 nm). The resulting solutions were stirred for 30 min at room temperature and then centrifuged at 10 000 rpm and washed with fresh MeOH three times. The ZIF-8 products were dried overnight at 100 °C in an oven.

Characterization

X-ray diffraction (XRD) measurements were performed using an Empyrean PANalytical diffractometer with a Cu-K_α radiation source (λ = 1.5406 Å). Data were collected in the 2θ range from 2.5° to 40° and at a scanning rate of 0.01° s^{-1}. Thermogravimetric analysis (TGA) was carried out with a Mettler Toledo DSC-1 Star System at a heating rate of 10 °C min^{-1} up to 800 °C under an airflow of 80 cm^3(STP) min^{-1}. Scanning electron microscopy (SEM) images of the buckypapers were obtained with an FEI-Inspect F50 microscope operating at a voltage of 10 kV. SEM was also applied to evaluate the morphology and particle size distribution of ZIF-8 particles using ImageJ software. All samples were coated with Au/Pd under vacuum conditions prior to analysis. Raman analysis was performed using a WiTec Alpha300 confocal Raman microscope with a 488 nm laser excitation beam. The intensities of the characteristic bands (D and G) were used to evaluate the SWCNTs. Mercury porosimetry was performed with a Micromeritics Autopore IV porosimeter (operating in the 28–60 000 psia range) at room temperature. Brunauer–Emmett–Teller (BET) specific surface area, specific pore volumes and Barrett–Joyner–Halenda (BJH) pore size distribution were obtained from N_2 adsorption data acquired at −196 °C using a Micromeritics Tristar 3000 after outgassing the samples at 200 °C for 9 h.

The curve of pressure drop *versus* air flow rate was obtained with a controlled flow of air (Bronkhorst MV104) forced through various samples of the membrane placed between two perforated metallic discs with inner diameter of 13.3 mm. The pressure drop was measured with a digital pressure meter (Digitron 2088P, 0–100 kPa). The flow was progressively increased until the buckypaper filter broke, which occurred at pressures of *ca* 35 kPa.

The efficiency of the buckypaper as a particle gas filter was determined at room temperature with a condensation particle counter (TSI 3782; this allows a particle count from 0 to ≥5 × 10^4 cm^{-3} with a limit of detection of 10 nm particle size) and a chamber in which a constant concentration of a polydisperse NaCl aerosol was maintained (mean particle diameter *ca* 85 nm in number, *ca* 270 nm in mass, *ca* 6 × 10^4 cm^{-3}). The aerosol was generated with a TOPAS ATM 226 coupled to a large dry-air stream. The air flow rate through the filter was 0.6 L(STP) min^{-1}. The filter had in this case a greater active area (40 mm in diameter) to allow the flow/absolute pressure conditions required by

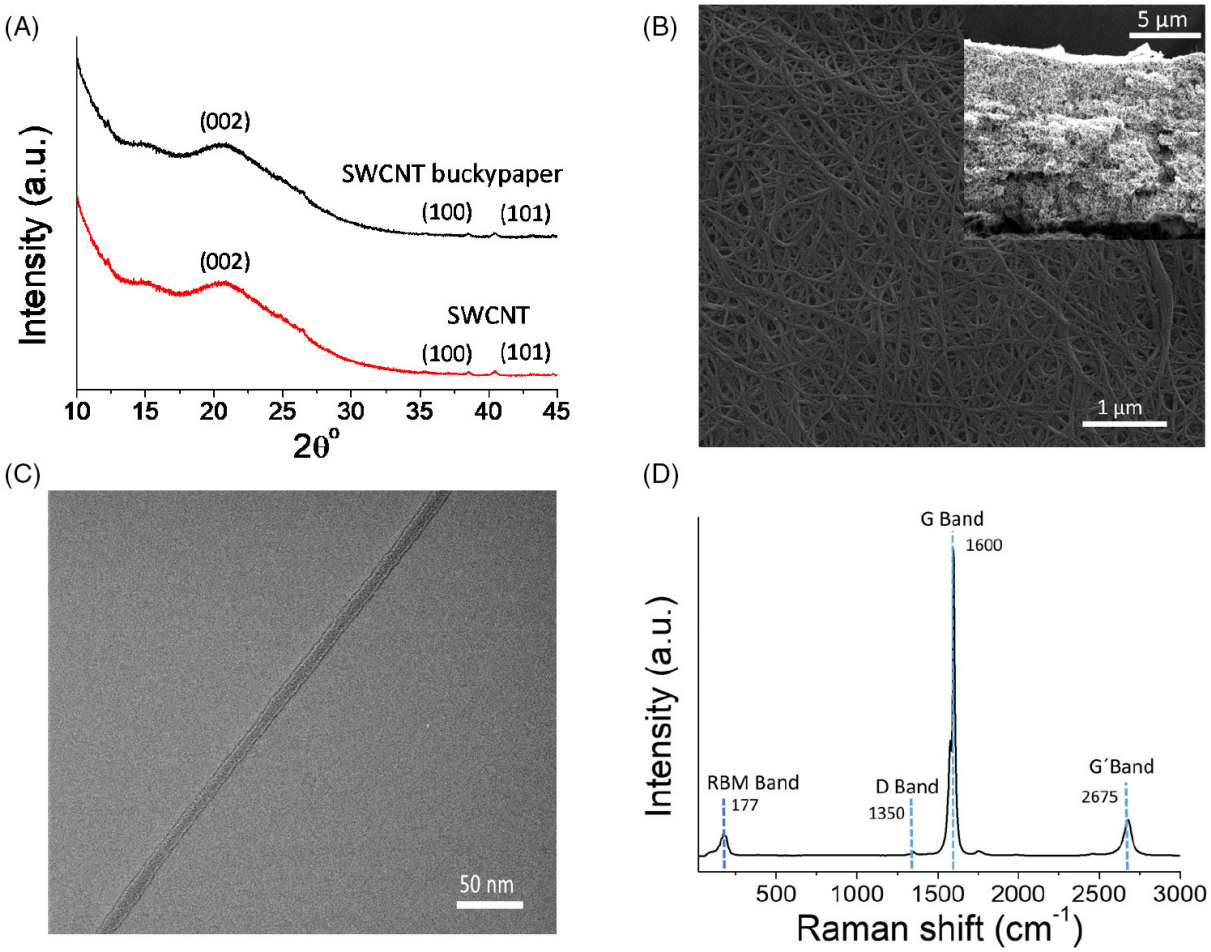

Figure 1. SWCNT basic characterization: XRD patterns (A), SEM image with inset showing cross-section (B), TEM image of a single SWCNT (C) and Raman spectrum (D).

Journal of Chemical Technology and Biotechnology published by John Wiley & Sons Ltd on behalf of Society of Chemical Industry (SCI).

the condensation particle counter. It was supported by a porous sintered steel disc to avoid the breakage of the membrane at the working pressure drop.

The liquid-phase membrane filtration performance was determined at room temperature using a dead-end membrane module (Sterlitech HP4750) working at a pressure drop of 2.5 bar and with nanoparticles of ZIF-8, with sizes of 30, 50 and 120 nm, suspended in water in a concentration of 10 mg L^{-1}. The effective area of the membrane was 12 cm^2 and the feed volume was 250 mL. Three different membrane samples were used in the same conditions to calculate the error bars shown in the results. In these conditions, the membrane water permeance and rejection parameters were calculated according to Eqns (3) and (4):

$$\text{Permeance} = \frac{V}{\Delta P A t} \tag{3}$$

$$\text{Rejection}\,(\%) = \left(1 - \frac{C_{\text{permeate}}}{C_{\text{retentate}}}\right) \times 100 \tag{4}$$

where V is the permeate volume (L), A is the membrane area (m^2), t is the time for permeate collection (h), C_{permeate} and $C_{\text{retentate}}$ the concentrations in the permeate and the retentate, respectively, and ΔP is the pressure across the membrane (bar). The ZIF-8 concentrations of retentate and permeate were measured using a UV spectrophotometer (Jasco V-670) at a wavelength of 203 nm.

RESULTS AND DISCUSSION

SWCNT, ZIF-8 and membrane characterization

The SWCNTs were used as received, but they were characterized to confirm the specifications given by the supplier. TGA (Fig. S1) shows thermal stability up to 500 °C which corresponds with the data provided by the supplier. Figure 1(A) depicts the characteristic XRD peaks at 2θ values of 20.8°, 38.6° and 40.5° corresponding to the (002), (100) and (101) crystal planes typical of the material.[51]

SEM images (Fig. 1(B)) show a wide CNT distribution with a mean diameter of *ca* 30 nm forming a homogeneous layer *ca* 15 µm thick (inset in Fig. 1(B)). This CNT diameter differs from the supplier data (diameter of 1.2–2.0 nm by optical absorption and 5 µm length). This significant difference is attributed to agglomeration of SWCNTs linked to the thickness added by the metal coating used for SEM sample preparation. In fact, transmission electron microscopy (TEM) characterization (Fig. 1(C)) allows confirming a mean diameter of *ca* 6 nm that is more similar to the expected diameter aforesaid, but SWCNT bundles still can be observed which can explain the verified discrepancy.

The Raman spectrum (Fig. 1(D)) shows the radial breathing mode (RBM) at 177 cm^{-1}. The graphene band (G band) was observed at 1600 cm^{-1} and its broadening is related to the small diameter of the SWCNTs. The low intensity of the D band at 1350 cm^{-1} signifies a low number of defects.[52] Also can be seen is the second-order G band (G′ band) at 2675 cm^{-1}. The RBM band is sensitive to the nanotube diameter according to Eqn (5)[53]:

$$\omega_{\text{RBM}} = \frac{A}{d} + B \tag{5}$$

where ω_{RBM} is the vibration frequency of the RBM band in cm^{-1}, d is the nanotube diameter in nm and A and B are constants with values of 234 cm^{-1} nm and 10 cm^{-1}, respectively. With this expression a diameter of 1.4 nm was obtained, which better agrees with the 1.2–2.0 nm specified by the supplier.

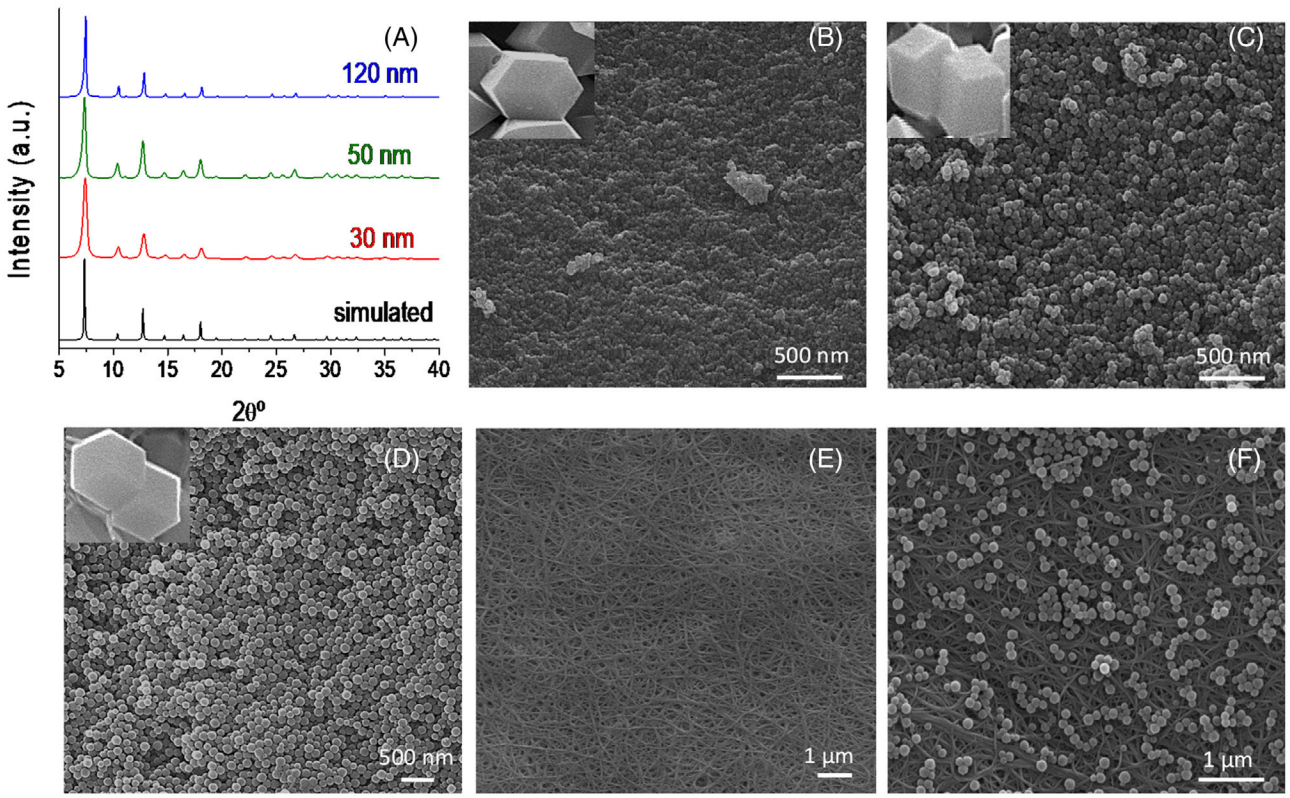

Figure 2. XRD patterns of ZIF-8 particles (A). SEM images of ZIF-8 particles: 30 nm (B), 50 nm (C) and 120 nm (D), with insets showing higher magnification images. SEM images of SWCNT buckypaper before (E) and after filtration (F).

Journal of Chemical Technology and Biotechnology published by John Wiley & Sons Ltd on behalf of Society of Chemical Industry (SCI).

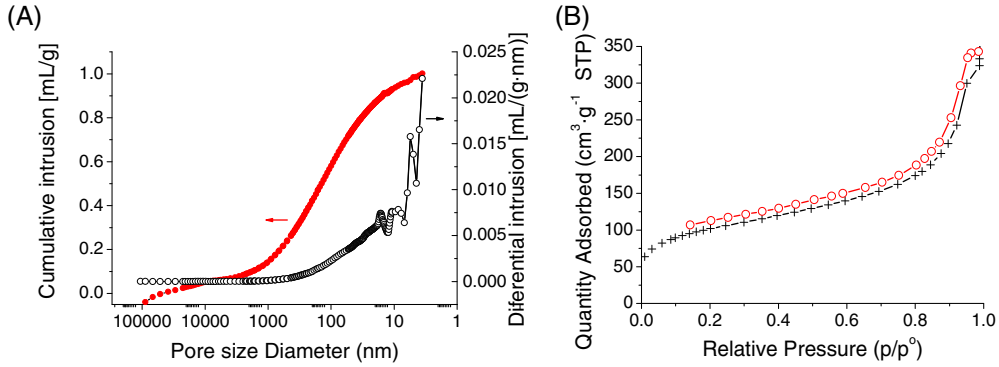

Figure 3. SWCNT buckypapers: mercury porosimetry analysis at room temperature (A) and nitrogen adsorption and desorption isotherms measured at −196 °C (B).

Table 1. Air performance comparison with CNT and SWCNT filters

Structure	Thickness of filter (μm)	Pressure drop (kPa)	Filtration efficiency (%)	Quality factor (kPa^{-1})	Ref.
MWNT-coated filter	202	2.99	99.9976 (50–100 nm)	3.56	13
Free-standing SWCNT film	0.12	1.5	99.997 (44 nm)	147	58
Aligned CNT sheet	25	0.147	99.98 (0.01–0.3 μm)	57.9	59
CNT/metallic fiber filter	-	0.115	93.8 (130 nm)	24.18	23
Three-dimensional CNT scaffolds	500	25	99 (0.3–2 μm)	0.18	60
CNT-coated glass fiber filter	200	0.080	33.3 (100–120 nm)	5.06	61
CNT/quartz-fiber filter	450	0.84	99.974 (100–300 nm)	9.89	62
CNT/quartz fiber filter nanostructured	430	0.435	99.9959 (64–88 nm)	23.21	63
CNF/sintered nickel microfibrous matrix	430	0.7	79–80 (90–7500 nm)	2–4	64
SWCNT buckypaper	15	34.2	99.9991	0.34	This work

The XRD patterns (Fig. 2(A)) of the ZIF-8 particles prepared reveal their purity and crystalline structure. The ZIF-8 nanosized crystals, prepared under different synthesis conditions, show the expected rombododecahedral morphology via SEM with narrow particle size distributions of *ca* 30 ± 8, 50 ± 5 and 120 ± 12 nm (Figs 2(B)–(D)). A smaller particle size is obtained at a higher dilution of the metal salt and the ligand as previously observed,[54] which may be related to a lower crystallization rate. These nanoparticles will be used as reference solutes for the subsequent UF experiments. As far as we know, this is the first time that a MOF has been used as solute to characterize membrane performance. In fact, ZIF-8, as well as other MOFs, can be synthesized at a given narrow particle size distribution by controlling the synthesis conditions, as demonstrated above.

The self-supported SWCNT buckypaper membranes were applied to aerosol/air filtration. In this context, porosity and pore size distribution are important characteristics that affect the filter performance. In consequence, the characterization of the buckypapers by mercury porosimetry and nitrogen adsorption was carried out to determine the presence of macro-, meso- and micropores.

In the pore size distribution obtained with mercury porosimetry (Fig. 3(A)), a broad peak can be observed that ranges pore sizes from 20 to 1000 nm, with macroporous (larger than 50 nm) and mesoporous (in the 2–50 nm range) peaks at 100, 15 and 5 nm. These pores are mainly due to the empty spaces created by the agglomerates of SWCNTs. The calculated porosity is about 49%.

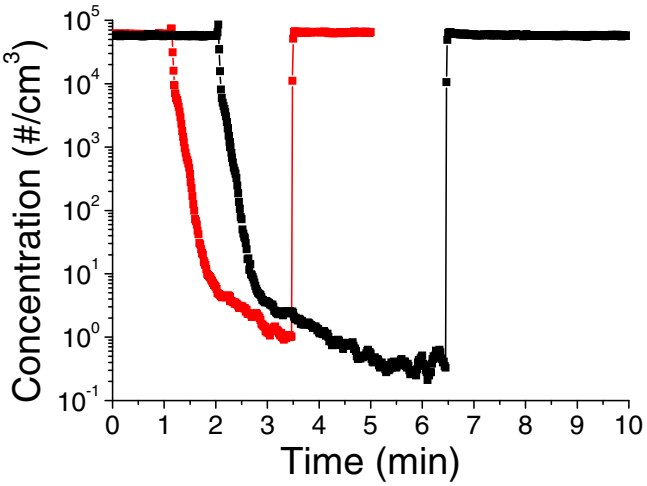

Figure 4. Evolution of the total concentration of NaCl particles downstream of the membrane in two independent tests carried out with the SWCNT buckypaper sample after commutation of sampling lines.

The nitrogen adsorption and desorption curves of the buckypapers show a characteristic appearance of a type IV isotherm, according to the IUPAC classification, with a hysteresis at high relative pressures related to capillary condensation inside the 5–15 nm mesopores and the relatively small 100 nm macropores, both

Journal of Chemical Technology and Biotechnology published by John Wiley & Sons Ltd on behalf of Society of Chemical Industry (SCI).

present between the SWCNTs (Fig. 3(B)). In addition, the isotherm has a filling of pores at low pressures ($P/P_0 < 0.1$), indicating the presence of micropores that have been attributed to channels between individual nanotubes within CNT bundles.[55] A BET specific surface area value of 362 ± 3 $m^2\ g^{-1}$ was achieved, lower than those previously reported when using Triton X-100 to prepare SWCNT buckypapers (642–790 $m^2\ g^{-1}$),[56] but within the wide range reported for this material (i.e. 96–790 $m^2\ g^{-1}$).[13,57,56] A pore volume of 0.50 $cm^3\ g^{-1}$ was measured at $P/P_0 < 0.987$. The *t*-plot analysis of nitrogen isotherm gives a micropore volume of 0.04 $cm^3\ g^{-1}$ and a micropore specific area of 97 $m^2\ g^{-1}$, confirming the presence of micropores. BJH analysis shows a wide range of mesopores in the 2–50 nm range (Fig. S2).

The air permeation characterization resulted in a permeance of 241 ± 40 $m^3\ m^{-2}\ h^{-1}\ bar^{-1}$ at a pressure drops of 34.2 kPa (Fig. S3). This pressure drop significantly overpasses those previously reported giving rise to a lower QF value of 0.34 kPa^{-1}. However, the filtration efficiency (99.9991%) is higher than those obtained with other CNT and multiwall CNT filters (Table 1). The large thickness of the SWCNT membrane prepared here (*ca* 15 μm) is the predominant cause of the increase in the pressure drop value, since in our case all the thickness corresponds to SWCNTs, whilst in the others the CNTs constitute a thin layer over the very permeable support which provides the majority of the thickness.

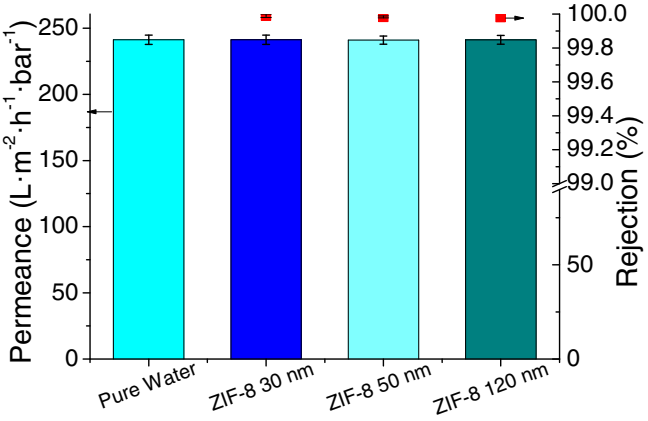

Figure 5. Permeance and rejection of the SWCNT buckypaper when separating MOF suspensions with ZIF-8 of 30, 50 and 120 nm in size. The error bars shown correspond to averaging results coming from three different membranes.

During air filtration testing (Fig. 4), the gas in the chamber was alternately sampled through the membrane and bypassed to monitor the particle concentration in the feed stream. In these conditions, the efficiency was calculated as the ratio of the measured concentrations. The test started with the continuous measurement of the chamber concentration, and after 2 min of constant concentration the lines were switched. After a transient period, the concentration downstream of the membrane oscillated between 0.2 and 0.5 cm^{-3}, which resulted in the efficiency above mentioned of around 99.9991 ± 0.0001% (the error coming from the averaging of the two independent experiments shown in Fig. 4). Note that this efficiency is essentially determined by the initial concentration allowed by the instrument, rather than by the final one, which in fact is averaged in time (intermittent signal). Finally, the sampling lines were again switched to check the stability of the chamber concentration throughout the test. The low concentration downstream of the membrane prevented the measurement of the particle size distribution and thus the dependence of the efficiency *versus* diameter.

Water filtration performance

UF corresponds to the filtration of particles with sizes in the 20–100 nm range,[25] which can be of interest when nanoplastics are the targeted type of pollutant.[1] Thus the water-phase semi-continuous experiments carried out here with suspensions containing ZIF-8 nanoparticles of 30 to 120 nm fall approximately in the field of UF. Moreover, trying to minimize any eventual fouling effect on the membrane with the smallest MOFs, the experiments were performed with the same sample starting with the largest ZIF-8 particles and ending with the smallest ones. Figure 5 shows similar values of water permeance of 241.2 ± 3.3 L $m^{-2}\ h^{-1}\ bar^{-1}$ and rejections of 99.99% with all the ZIF-8 particle sizes tested here. These high values are in general larger than those previously reported, as presented in Table 2. They are in agreement with the SEM images in Figs 2(E) and (F) illustrating the great capability of the membranes to reject nanometric solutes. Interestingly, the UF conditions applied did not seem to create large ZIF-8 agglomerates

Table 2. Permeance and rejection compilation of different CNT-based membranes

Membrane	Permeance (L $m^{-2}\ h^{-1}\ bar^{-1}$)	Application[a]	Rejection (%)	Ref.
CNTs-PES	9.7	NF	87.3	65
CNTs-PVDF	5.0	NF	50–60	66
GO coated VA CNTs	5.0	NF	44.9	67
PA coated VA CNTs	4.0	NF	64.8	67
CNTs-PP	36.8 (L $m^{-2}\ h^{-1}$)[b]	MD	99.9	68
CNTs-PTFE	69 (L $m^{-2}\ h^{-1}$)[b]	MD	93	69
CNTs-PVDF	19.1 (L $m^{-2}\ h^{-1}$)[b]	MD	93	70
CNTs-YSZ	36	MF	100	71
CNTs-PSF	47.5	UF	97.4	72
CNTs-mullite	8.1	UF	62.9	73
CNTs-Al_2O_3	≥4.5	MF	≥75	74
SWCNT buckypaper	241	UF (ZIF-8 30 nm)	99.99	This work

[a] NF, nanofiltration; UF, ultrafiltration; MF, microfiltration; MD, membrane distillation.
[b] Applied pressure not available.

Journal of Chemical Technology and Biotechnology published by John Wiley & Sons Ltd on behalf of Society of Chemical Industry (SCI).

on the SWCNT buckypaper. And the ZIF-8 particles did not seem to penetrate into the membrane structure, suggesting an easy cleaning and reuse. In addition, this demonstrates that the use of these membranes constitutes an efficient way to remove MOF nanoparticles (and analogous polymeric pollutants such as the abovementioned nanoplastics) suspended in water down to 30 nm in diameter. In fact, the control of ZIF-8 crystallization to produce nanoparticles with homogeneous particle size distributions in the 30–120 range size allows the use of such nanoparticles as a reference solute for testing the application of SWCNT buckypapers to separation by membrane UF.

Besides the separation performance in gas and liquid phases, there are other advantages that buckypapers could provide during UF. They can show better resistance to temperature and chemical agents than other types of polymeric membranes,[31] SWCNTs can help to eliminate organic micropollutants by adsorption during UF[75] and CNTs in composite membranes have shown high antibacterial activity so they may have a high potential for avoiding biofouling and in general fouling by biomolecules.[76] Finally, the inherent conductivity of membranes containing CNTs could help in the use of an electrochemical stimulus to reduce fouling.[22]

CONCLUSIONS

We have reported a simple technique for the rapid fabrication of self-supported SWCNT buckypaper membranes with a filtration method resulting in an excellent performance in both air and water filtration. The filters exhibit an air permeation of 241 m^3m^{-2} bar^{-1} h^{-1} and a pressure drop of 34.2 kPa. This value, even if higher than that of some previously reported membranes, is the first one obtained without any kind of support together with a filtration efficiency of 99.9991% calculated from the ratio between the concentrations of NaCl particles at both sides of the membrane.

The performance of the membranes was also tested in water UF of suspensions containing 30–120 nm nanoparticles of ZIF-8 (e.g. simulating polymeric pollutants such as nanoplastics) achieving water permeances of 241 L m^{-2} h^{-1} bar^{-1} with rejections of 99.99% with all three particle sizes. These results suggest the use of the SWCNT membrane in the UF range and the use of MOFs as reference solutes of well-controlled particle sizes. Finally, the successive experiments done with the same CNT buckypaper samples (two sequential experiments in gas-phase application with the same sample and three sequential experiments in liquid phase with each different ZIF-8 particle size with three different samples) suggest that the membranes have good reliability and reproducibility, even if long-term experiments would be desirable as future work.

ACKNOWLEDGEMENTS

Financial support from the Aragón Government is gratefully acknowledged (T43_20R). VB-S acknowledges grant BES-2017-080209 funded by MCIN/AEI/10.13039/501100011033 and by 'ESF investing in your future'. The authors acknowledge the use of the Servicio General de Apoyo a la Investigación-SAI and the use of instrumentation as well as the technical advice provided by the National Facility ELECMI ICTS, node Laboratorio de Microscopias Avanzadas at the University of Zaragoza.

SUPPORTING INFORMATION

Supporting information may be found in the online version of this article.

REFERENCES

1 Malankowska M, Echaide-Gorriz C and Coronas J, Microplastics in marine environment: a review on sources, classification, and potential remediation by membrane technology. *Environ Sci Water Res Technol* **7**:243–258 (2021).
2 Fischer T, Wheat yield losses in India due to ozone and aerosol pollution and their alleviation: a critical review. *Outlook Agric* **48**:181–189 (2019).
3 Shahidi D, Roy R and Azzouz A, Advances in catalytic oxidation of organic pollutants: prospects for thorough mineralization by natural clay catalysts. *Appl Catal Environ* **174–175**:277–292 (2015).
4 Kamal MS, Razzak SA and Hossain MM, Catalytic oxidation of volatile organic compounds (VOCs): a review. *Atmos Environ* **140**:117–134 (2016).
5 Lu F and Astruc D, Nanocatalysts and other nanomaterials for water remediation from organic pollutants. *Coord Chem Rev* **408**:213180 (2020).
6 Parmar GR and Rao NN, Emerging control technologies for volatile organic compounds. *Crit Rev Environ Sci Technol* **39**:41–78 (2009).
7 Aalto P, Hämeri K, Paatero P, Kulmala M, Bellander T, Berglind N *et al.*, Aerosol particle number concentration measurements in five European cities using TSI-3022 condensation particle counter over a three-year period during health effects of air pollution on susceptible subpopulations. *J Air Waste Manag Assoc* **55**:1064–1076 (2005).
8 Zwozdziak A, Gini MI, Samek L, Rogula-Kozlowska W, Sowka I and Eleftheriadis K, Implications of the aerosol size distribution modal structure of trace and major elements on human exposure, inhaled dose and relevance to the PM2.5 and PM10 metrics in a European pollution hotspot urban area. *J Aerosol Sci* **103**:38–52 (2017).
9 Mannucci PM, Harari S, Martinelli I and Franchini M, Effects on health of air pollution: a narrative review. *Intern Emerg Med* **10**:657–662 (2015).
10 Brook RD, Rajagopalan S, Pope CA, Brook JR, Bhatnagar A, Diez-Roux AV *et al.*, Particulate matter air pollution and cardiovascular disease: an update to the scientific statement from the American heart association. *Circulation* **121**:2331–2378 (2010).
11 Barhate RS and Ramakrishna S, Nanofibrous filtering media: filtration problems and solutions from tiny materials. *J Membr Sci* **296**:1–8 (2007).
12 Zhang R and Wei F, High-efficiency particulate air filters based on carbon nanotubes, in *Nanotube Superfiber Materials: Science, Manufacturing, Commercialization*, 2nd edn. Elsevier Inc, Norwich, pp. 643–666 (2019).
13 Viswanathan G, Kane DB and Lipowicz PJ, High efficiency fine particulate filtration using carbon nanotube coatings. *Adv Mater* **16**:2045–2049 (2004).
14 Tang M, Hu J, Liang Y and Pui DYH, Pressure drop, penetration and quality factor of filter paper containing nanofibers. *Text Res J* **87**:498–508 (2017).
15 Kim HJ, Park SJ, Kim DI, Lee S, Kwon OS and Kim IK, Moisture effect on particulate matter filtration performance using electro-spun nanofibers including density functional theory analysis. *Sci Rep* **9**:7015 (2019).
16 Maze B, Vahedi Tafreshi H, Wang Q and Pourdeyhimi B, A simulation of unsteady-state filtration via nanofiber media at reduced operating pressures. *J Aerosol Sci* **38**:550–571 (2007).
17 Sabzehmeidani MM, Mahnaee S, Ghaedi M, Heidari H and Roy VAL, Carbon based materials: a review of adsorbents for inorganic and organic compounds. *Mater Adv* **2**:598–627 (2021).
18 Sharma A, Jindal J, Mittal A, Kumari K, Maken S, Kumar N. Carbon materials as CO_2 adsorbents: a review. *Environ Chem Lett* 2021;**19**:875–910.
19 Vetrivel R, Navinselvakumar C and Samuel Ratna Kumar PS, Carbon nanotubes and its applications – a review. *Int J Mech Prod Eng Res Dev* **8**:288–293 (2018).
20 Gibson P, Schreuder-Gibson H and Rivin D, Transport properties of porous membranes based on electrospun nanofibers. *Colloids Surf A* **187**:469–481 (2001).
21 Balamurugan R, Sundarrajan S and Ramakrishna S, Recent trends in nanofibrous membranes and their suitability for air and water filtrations. *Membranes (Basel)* **1**:232–248 (2011).
22 Rashid MHO and Ralph SF, Carbon nanotube membranes: synthesis, properties, and future filtration applications. *Nanomaterials* **7**:99 (2017).
23 Park SJ and Lee DG, Performance improvement of micron-sized fibrous metal filters by direct growth of carbon nanotubes. *Carbon* **44**:1930–1935 (2006).
24 Ahuja S, *Chemistry and Water: The Science behind Sustaining the World's Most Crucial Resource*, 1st edn. Elsevier, Amsterdam (2016).

Journal of Chemical Technology and Biotechnology published by John Wiley & Sons Ltd on behalf of Society of Chemical Industry (SCI).

25 Warsinger DM, Chakraborty S, Tow EW, Plumlee MH, Bellona C, Loutatidou S *et al.*, A review of polymeric membranes and processes for potable water reuse. *Prog Polym Sci* **81**:209–237 (2018).
26 Andrady AL, Microplastics in the marine environment. *Mar Pollut Bull* **62**:1596–1605 (2011).
27 Jambeck JR, Andrady A, Geyer R, Narayan R, Perryman M, Siegler T *et al.*, Plastic waste inputs from land into the ocean. *Science* **347**: 768–771 (2015).
28 Pyrzynska K, Carbon nanotubes as a new solid-phase extraction material for removal and enrichment of organic pollutants in water. *Sep Purif Rev* **37**:372–389 (2008).
29 Tang Y, Zhang S, Su Y, Wu D, Zhao Y and Xie B, Removal of microplastics from aqueous solutions by magnetic carbon nanotubes. *Chem Eng J* **406**:126804 (2021).
30 Popov VN, Carbon nanotubes: properties and application. *Mater Sci Eng R* **43**:61–102 (2004).
31 Upadhyayula VKK, Deng S, Mitchell MC and Smith GB, Application of carbon nanotube technology for removal of contaminants in drinking water: a review. *Sci Total Environ* **408**:1–13 (2009).
32 Tofighy MA and Mohammadi T, Permanent hard water softening using carbon nanotube sheets. *Desalination* **268**:208–213 (2011).
33 Goh PS, Ismail AF and Ng BC, Carbon nanotubes for desalination: performance evaluation and current hurdles. *Desalination* **308**:2–14 (2013).
34 Lee C and Baik S, Vertically-aligned carbon nano-tube membrane filters with superhydrophobicity and superoleophilicity. *Carbon* **48**: 2192–2197 (2010).
35 Gupta VK and Saleh TA, Adsorption on carbon nanotubes. *A B Ion Exch Adsorpt Solvent Extr* **357**:111–120 (2013).
36 Ma L, Dong X, Chen M, Zhu L, Wang C, Yang F *et al.*, Fabrication and water treatment application of carbon nanotubes (CNTs)-based composite membranes: a review. *Membranes (Basel)* **7**:16 (2017).
37 Ribeiro B, Botelho EC, Costa ML and Bandeira CF, Carbon nanotube buckypaper reinforced polymer composites: a review. *Polimeros* **27**:247–255 (2017).
38 Yang X, Lee J, Yuan L, Chae SR, Peterson VK, Minett AI *et al.*, Removal of natural organic matter in water using functionalised carbon nanotube buckypaper. *Carbon* **59**:160–166 (2013).
39 Falcaro P, Ricco R, Doherty CM, Liang K, Hill AJ and Styles MJ, MOF positioning technology and device fabrication. *Chem Soc Rev* **43**: 5513–5560 (2014).
40 Sorribas S, Gorgojo P, Téllez C, Coronas J and Livingston AG, High flux thin film nanocomposite membranes based on metal-organic frameworks for organic solvent nanofiltration. *J Am Chem Soc* **135**: 15201–15208 (2013).
41 Mendes RF, Figueira F, Leite JP, Gales L and Almeida Paz FA, Metal-organic frameworks: a future toolbox for biomedicine? *Chem Soc Rev* **49**:9121–9153 (2020).
42 Etxeberria-Benavides M, Johnson T, Cao S, Zornoza B, Coronas J, Sanchez-Lainez J *et al.*, PBI mixed matrix hollow fiber membrane: influence of ZIF-8 filler over H_2/CO_2 separation performance at high temperature and pressure. *Sep Purif Technol* **237**:116347 (2020).
43 Singh N, Qutub S and Khashab NM, Biocompatibility and biodegradability of metal organic frameworks for biomedical applications. *J Mater Chem B* **9**:5925–5934 (2021).
44 Hao F and Yan XP, Nano-sized zeolite-like metal-organic frameworks induced hematological effects on red blood cell. *J Hazard Mater* **424**:127353 (2022).
45 Li Y, Shang S, Shang J and Wang WX, Toxicity assessment and underlying mechanisms of multiple metal organic frameworks using the green algae *Chlamydomonas reinhardtii* model. *Environ Pollut* **291**: 118199 (2021).
46 Li D, Zhou Q, Hu X, Mu L, Zeng H and Luo J, Environmental decomposition and remodeled phytotoxicity of framework-based nanomaterials. *J Hazard Mater* **422**:126846 (2022).
47 Rojas JA, Ardila-Rodríguez LA, Diniz MF, Gonçalves M, Ribeiro B and Rezende MC, Optimization of triton X-100 removal and ultrasound probe parameters in the preparation of multiwalled carbon nanotube buckypaper. *Mater Des* **166**:107612 (2019).
48 Chew SY, Ng SH, Wang J, Novák P, Krumeich F, Chou SL *et al.*, Flexible free-standing carbon nanotube films for model lithium-ion batteries. *Carbon* **47**:2976–2983 (2009).
49 Cravillon J, Münzer S, Lohmeier SJ, Feldhoff A, Huber K and Wiebcke M, Rapid room-temperature synthesis and characterization of nanocrystals of a prototypical zeolitic imidazolate framework. *Chem Mater* **21**:1410–1412 (2009).
50 García-Palacín M, Martínez JI, Paseta L, Deacon A, Johnson T, Malankowska M *et al.*, Sized-controlled ZIF-8 nanoparticle synthesis from recycled mother liquors: environmental impact assessment. *ACS Sustain Chem Eng* **8**:2973–2980 (2020).
51 Cao A, Xu C, Liang J, Wu D and Wei B, X-ray diffraction characterization on the alignment degree of carbon nanotubes. *Chem Phys Lett* **344**: 13–17 (2001).
52 Kalbac M, Hsieh YP, Farhat H, Kavan L, Hofmann M, Kong J *et al.*, Defects in individual semiconducting single wall carbon nanotubes: Raman spectroscopic and in situ Raman spectroelectrochemical study. *Nano Lett* **10**:4619–4626 (2010).
53 Costa S, Borowiak-Palen E, Kruszyñska M, Bachmatiuk A and Kaleńczuk RJ, Characterization of carbon nanotubes by Raman spectroscopy. *Mater Sci Pol* **26**:433–441 (2008).
54 Marshall CR, Staudhammer SA and Brozek CK, Size control over metal-organic framework porous nanocrystals. *Chem Sci* **10**:9396–9408 (2019).
55 Sweetman LJ, Nghiem L, Chironi I, Triani G, in het Panhuis M and Ralph SF, Synthesis, properties and water permeability of SWNT buckypapers. *J Mater Chem* **22**:13800–13810 (2012).
56 Muramatsu H, Hayashi T, Kim YA, Shimamoto D, Kim YJ, Tantrakarn K *et al.*, Pore structure and oxidation stability of double-walled carbon nanotube-derived bucky paper. *Chem Phys Lett* **414**:444–448 (2005).
57 Inoue S, Ichikuni N, Suzuki T, Uematsu T and Kaneko K, Capillary condensation of N_2 on multiwall carbon nanotubes. *J Phys Chem B* **102**:1–4 (1998).
58 Nasibulin AG, Kaskela A, Mustonen K, Anisimov AS, Ruiz V, Kivistö S *et al.*, Multifunctional free-standing single-walled carbon nanotube films. *ACS Nano* **5**:3214–3221 (2011).
59 Yildiz O and Bradford PD, Aligned carbon nanotube sheet high efficiency particulate air filters. *Carbon* **64**:295–304 (2013).
60 Halonen N, Rautio A, Leino A, Kyllo T, Huuhtanen M, Keiski RL *et al.*, Three-dimensional carbon nanotube catalyst support membranes. *ACS Nano* **4**:2003–2008 (2010).
61 Park KT and Hwang J, Filtration and inactivation of aerosolized bacteriophage MS2 by a CNT air filter fabricated using electro-aerodynamic deposition. *Carbon* **75**:401–410 (2014).
62 Li P, Zong Y, Zhang Y, Yang M, Zhang R, Li S *et al.*, In situ fabrication of depth-type hierarchical CNT/quartz fiber filters for high efficiency filtration of sub-micron aerosols and high water repellency. *Nanoscale* **5**:3367–3372 (2013).
63 Li P, Wang C, Li Z, Zong Y, Zhang Y, Yang X *et al.*, Hierarchical carbon-nanotube/quartz-fiber films with gradient nanostructures for high efficiency and long service life air filters. *RSC Adv* **4**:54115–54121 (2014).
64 Karwa AN and Tatarchuk BJ, Aerosol filtration enhancement using carbon nanostructures synthesized within a sintered nickel microfibrous matrix. *Sep Purif Technol* **87**:84–94 (2012).
65 Wang L, Song X, Wang T, Wang S, Wang Z and Gao C, Fabrication and characterization of polyethersulfone/carbon nanotubes (PES/CNTs) based mixed matrix membranes (MMMs) for nanofiltration application. *Appl Surf Sci* **2015**:118–125 (2015).
66 Madaeni SS, Zinadini S and Vatanpour V, Preparation of superhydrophobic nanofiltration membrane by embedding multiwalled carbon nanotube and polydimethylsiloxane in pores of microfiltration membrane. *Sep Purif Technol* **111**:98–107 (2013).
67 Baek Y, Seo DK, Choi JH, Lee B, Kim YH, Park SM *et al.*, Improvement of vertically aligned carbon nanotube membranes: desalination potential, flux enhancement and scale-up. *Desalin Water Treat* **57**:28133–28140 (2016).
68 Roy S, Bhadra M and Mitra S, Enhanced desalination via functionalized carbon nanotube immobilized membrane in direct contact membrane distillation. *Sep Purif Technol* **136**:58–65 (2014).
69 Bhadra M, Roy S and Mitra S, Flux enhancement in direct contact membrane distillation by implementing carbon nanotube immobilized PTFE membrane. *Sep Purif Technol* **161**:136–143 (2016).
70 Gethard K, Sae-Khow O and Mitra S, Water desalination using carbon-nanotube-enhanced membrane distillation. *ACS Appl Mater Interfaces* **3**:110–114 (2011).
71 Chen X, Hong L, Xu Y and Ong ZW, Ceramic pore channels with inducted carbon nanotubes for removing oil from water. *ACS Appl Mater Interfaces* **4**:1909–1918 (2012).
72 Maphutha S, Moothi K, Meyyappan M and Iyuke SE, A carbon nanotube-infused polysulfone membrane with polyvinyl alcohol layer for treating oil-containing waste water. *Sci Rep* **3**:1509 (2013).

Journal of Chemical Technology and Biotechnology published by John Wiley & Sons Ltd on behalf of Society of Chemical Industry (SCI).

73 Ahmadzadeh Tofighy M and Mohammadi T, Nickel ions removal from water by two different morphologies of induced CNTs in mullite pore channels as adsorptive membrane. *Ceram Int* **41**:5464–5472 (2015).
74 Tofighy MA and Mohammadi T, Synthesis and characterization of ceramic/carbon nanotubes composite adsorptive membrane for copper ion removal from water. *Korean J Chem Eng* **32**:292–298 (2015).
75 Nguyen MN, Trinh PB, Burkhardt CJ and Schäfer AI, Incorporation of single-walled carbon nanotubes in ultrafiltration support structure for the removal of steroid hormone micropollutants. *Sep Purif Technol* **264**:1–13 (2021).
76 Ihsanullah, Carbon nanotube membranes for water purification: developments, challenges, and prospects for the future. *Sep Purif Technol* **209**:307–337 (2019).